Semi-mind controlled robots based on Reinforcement Learning for Indoor Application

Ilyes Naidji[1], Ahmed Tibermacine[1], Walid Guettala[1] and Imad Eddine Tibermacine[2]

[1]Department of Computer Science, University Mohamed Khider of Biskra, Algeria
[2] Department of Computer, Control and Management Engineering , Sapienza University of Rome, Italy

Abstract

This paper presents a solution to this challenge by introducing interactive feedback derived from brain signals to train robots using deep reinforcement learning, particularly in the context of indoor maze navigation. Our objective is to enhance the learning process in a human-robot interaction scenario by incorporating human emotion or attention feedback. To accomplish this, we empowered the robot to learn new tasks through a dynamic policy network based on human feedback, and we augmented this input with other sensor data, including LIDAR. Various experiments are conducted to compare the efficacy of manual feedback, brain signal feedback, and no brain signal feedback, employing diverse Reinforcement Learning models. Additionally, we explore different models for emotion classification, employing Graph Neural Network models and traditional deep learning models, and subsequently compare the outcomes.

Keywords

EEG, Deep Learning, Graph Neural Networks, Human-Robot Interaction

1. Introduction

Robotic applications have become indispensable across diverse fields such as rescue operations, medical assistance, and autonomous driving. Within the realm of mobile robotics, autonomous navigation stands out as a crucial research focus [1, 2], traditionally relying on map-building techniques like SLAM [3]. Nevertheless, there is a growing interest in mapless navigation, which establishes a direct link between sensory inputs and robot actions. While deep reinforcement learning (DRL) has made noteworthy advancements in autonomous navigation, the challenges of real-world training persist [4, 5].

In the presented paper [6], the authors introduce a novel model named the Correlated Attention Network (CAN) for multimodal emotion recognition[7, 8]. This model extends the attention-based recurrent neural network by integrating correlation calculations of different gated recurrent units, specifically targeting the correlation between EEG and eye movement signals[9]. Through the utilization of coordinated representation incorporating complementary features, the CAN model aims to achieve enhanced emotion classification accuracy. The experimental outcomes on three real-world datasets reveal that the proposed model outperforms existing state-of-the-art methods, achieving mean accuracies of 94.03% on the SEED dataset, 87.71% on the SEED IV dataset, and 88.51% and 85.62% for four classifications and two dichotomies on the DEAP dataset, respectively. The key contributions of the paper encompass the introduction of the CAN model, which combines deep-gated recurrent neural networks [10] with canonical correlation and an attention mechanism [11], and the exploration of coordinated representation in tasks related to multimodal emotion recognition[12].

The literature reviewed diverse approaches to autonomous robot navigation in unfamiliar environments[13, 14, 15]. Simultaneous Localization and Mapping (SLAM) algorithms, such as the one proposed in [16] and the lightweight OrthoSLAM algorithm [17], emphasize the simultaneous mapping and localization process. In [18], an innovative method is introduced, combining Hector SLAM with an Artificial Potential Field (APF) controller, specifically designed for indoor navigation in GPS-denied environments. The proposal in [19] advocates for a semantically rich graph representation in the context of indoor navigation. Additionally, research in [20, 21] explores end-to-end approaches utilizing Convolutional Neural Networks (CNNs) for autonomous robot navigation, particularly with RGB-D cameras[22].

Methods based on Deep Reinforcement Learning (DRL) are also explored, such as the fusion of deep reinforcement learning with Recurrent Neural Networks (RNNs)[23, 24**?**] for path selection discussed in [25]. In [26], an approach utilizing Deep Q-Network (DQN) for autonomous robot navigation with visual observations is presented, albeit relying on RGB-D cameras. Addressing collision avoidance and navigation, [27, 28] employ a Double Deep Q-Network (DDQN) approach. Lastly, [29] introduces an Asynchronous Advantage Actor-Critic net-

ICYRIME 2023: 8th International Conference of Yearly Reports on Informatics, Mathematics, and Engineering. Naples, July 28-31, 2023
ilyes.naidji@univ-biskra.dz (I. Naidji);
ahmed.tibermacine@univ-biskra.dz (A. Tibermacine);
walidguettala@gmail.com (W. Guettala);
tibermacine@diag.uniroma1.it (I. E. Tibermacine)

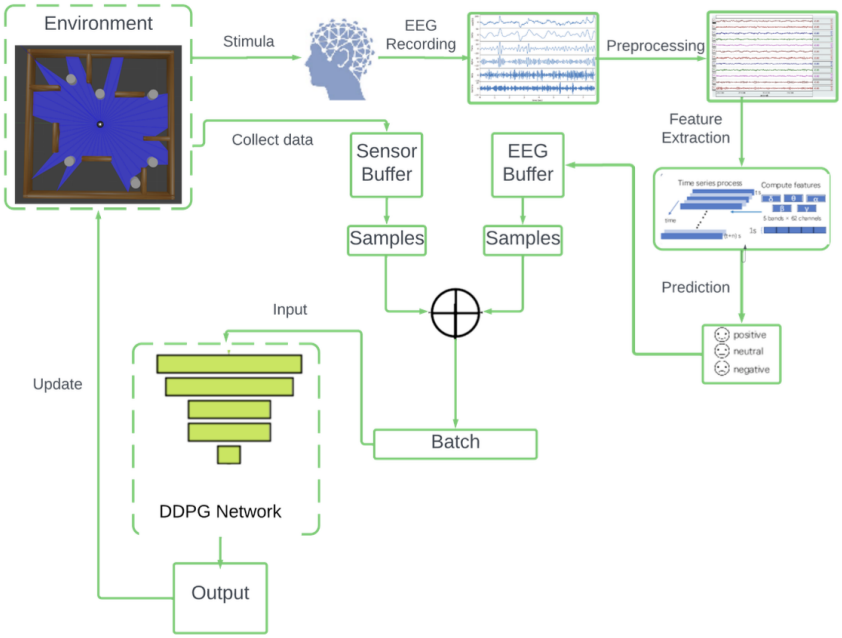

Figure 1: Global system design

work to enhance generalization and reduce learning time for indoor robot navigation.

These studies offer valuable insights into various techniques and algorithms employed in autonomous robot navigation, contributing to the comprehension of Simultaneous Localization and Mapping (SLAM), end-to-end strategies, Deep Reinforcement Learning (DRL), and collision avoidance methodologies.

2. Proposed model

2.1. Global System Design

The overarching design of this global system [Fig.1] adopts an AI perspective and consists of two principal components: the Brain Signal segment utilizing EEG and the DRL (Deep Reinforcement Learning) segment. The system architecture is defined by an environment featuring a maze with static obstacles representing maze walls and dynamic obstacles. A robot, guided by a DRL agent, endeavors to navigate through the maze with the goal of reaching a randomly generated red circular spot.

The DRL agent is reliant on two primary feedback signals for observations. The first is the EEG signal, portraying emotions like sadness, happiness, and neutrality. The second feedback is derived from a 2D LIDAR sensor, furnishing environmental information to the agent. Human interaction with the system is facilitated through a Brain-Computer Interface (BCI) setup. Users observe the simulation and gather EEG recordings. The collected EEG data undergoes preprocessing, feature extraction, and model prediction to categorize emotional states into three classes: sad, happy, and neutral.

Concurrently, the 2D LIDAR sensor data is amalgamated with the EEG data and serves as observations for the DRL agent. The agent acquires the ability to make optimal decisions and execute actions by assimilating the combined feedback, facilitating effective navigation through the maze. Various iterations of the system have been created, incorporating versions that exclusively rely on the 2D LIDAR sensor or concentrate solely on emotion feedback. Additionally, diverse noise types and persistent feedback mechanisms have been investigated to improve the overall performance of the system.

In the upcoming sections, specific Deep Reinforcement Learning (DRL) algorithms and their intricate functionalities will be elucidated, offering deeper insights into the operational and learning processes of the system.

3. EEG DATASET

3.1. Dataset Overview

The EEG dataset comprises recordings from 15 participants involved in the experiment. Each participant underwent three sessions on distinct days, and each session encompassed 24 trials. The film clips displayed during these trials were meticulously selected to elicit emotions such as happiness, sadness, fear, or a neutral emotional state. Consequently, the dataset encompasses four emotional classes: happiness, sadness, fear, and neutrality. The SEED IV dataset [30] offers an extensive compilation of EEG signals, with a specific emphasis on emotion recognition utilizing both EEG and eye movement data. This section provides an outline of the EEG segment within the SEED IV dataset utilized in this thesis. It encompasses details regarding the number of subjects, the film clips utilized, and the classes available. Additionally, information about the preprocessing of the EEG signals and the process of feature extraction is presented.

3.2. Brain Signal Feedback Part

This is a sub-system design from the global system which has 2 phases:

3.2.1. Phase 1

During this stage, the model, specifically the CNN model, is trained utilizing the SEED-IV dataset. We implemented the preprocessing and feature extraction methods outlined in the dataset section. For our model, predictions were made for four distinct classes. However, within our overarching system design, the classes of sadness and fear were amalgamated into a single class. Subsequently, the batches were converted into 2D images to be inputted into the CNN model. Alongside the CNN model trained in the train data loader, we also conducted experiments with alternative models, including advanced CNN architecture, LSTM, and ViT.

3.2.2. Phase 2

Upon completing the initial phase, we employ the trained weights and integrate them into our system as an offline model. This offline model encompasses a predetermined function that receives input from the BCI API, initially transforming the features to predict real-time human emotions. The predicted emotions are then stored in the EEG buffer. Subsequently, the EEG buffer is combined with the 2D lidar buffer, creating the sensor buffer and constituting the resultant batch.

3.2.3. Replacmnet of Emotion feedback

Concerning the brain signal feedback, it can be substituted with keyboard input involving humans as the source of feedback. In this scenario, users can input their emotional state, specifying whether they feel happy, sad, or neutral. Alternatively, the brain signal feedback system can be replaced with generated samples of emotional states adhering to a uniform distribution. In this approach, three variables govern the probability of each emotional event: happiness, sadness, and neutrality.

3.2.4. Classification Models Used For Emotion Dataset

We employed emotion classification as both a feedback system and an observation for deep reinforcement learning. This feedback offers insights into the individual's emotional state within the simulation. To accomplish this, we utilized diverse models for classifying brain signals into four categories: angry, sad, happy, or neutral.

3.2.5. Reward Function

The reward function comprises five versions denoted as A, B, C, D, and E. In Version A, lidar serves as the observation, while Version B utilizes a uniform distribution of emotion. Version C combines the uniform distribution of emotion with lidar, Version D relies solely on emotion, and Version E combines emotion with lidar. Our focus will be on the two principal reward functions, with the other three representing variations of these main ones.

The first reward function is a hybrid model that incorporates lidar and emotion as observations. The second reward function relies on a uniform distribution of emotion based on a specified probability. Additionally, there is a variable named 'constant' that is added to the reward when the robot successfully avoids collisions with obstacles. This constant value varies based on four types: Step-1, Step-2, Episode, and time, each defined in seconds. The constant is added according to one of these four types.

4. EXPERIMENTAL SETUP

4.1. Preprocessing and Feature Extraction

During the EEG preprocessing phase, several procedures were implemented to ready the data for subsequent analysis. These steps encompass downsampling the raw EEG data to a sampling rate of 200 Hz and applying a bandpass filter ranging from 1 Hz to 75 Hz to eliminate noise. Subsequent to the preprocessing stage, EEG feature extraction was conducted to capture pertinent information from the data. Extracted features include Power Spectral Density (PSD) and Differential Entropy (DE). PSD

quantifies the power distribution across five frequency bands, specifically Delta (1 Hz - 4 Hz), Theta (4 Hz - 8 Hz), Alpha (8 Hz - 14 Hz), Beta (14 Hz - 31 Hz), and Gamma (31 Hz - 50 Hz). Conversely, DE computes the differential entropy within each segment and across the aforementioned frequency bands.

4.1.1. Utilization of EEG Feature Data

The $eeg_feature_smooth$ directory within the SEED IV dataset served as the source for feature extraction, specifically employing the PSD and DE features. Data from each .mat file was loaded and transformed into a format suitable for model training. To optimize the training process, samples from each .mat file were concatenated into batches of size 128, where each batch contained EEG segments from different trials of the same subject. Furthermore, one label from the four emotional classes was assigned to each batch. These batches were then used to construct a dataloader, which was subsequently divided into training, validation, and testing sets with ratios of 0.8, 0.1, and 0.1, respectively. To introduce randomness into the training process, the dataset was shuffled.

By employing this methodology, our objective is to train a model capable of recognizing emotions based on EEG features extracted from the SEED IV dataset.

4.1.2. Simulation Feedback Data

The dataset utilized in this case study comprises environmental data acquired from a LIDAR sensor and feedback from an EEG (electroencephalogram) device. The LIDAR sensor supplies information about the surroundings, including distances to obstacles and the robot's orientation. Concurrently, the EEG device gauges the brain activity of the operator, offering feedback on their cognitive state.

5. Dynamical Graph Convolutional Neural Networks (DGCNN)

The DGCNN (Dynamical Graph Convolutional Neural Networks) model [**?**] is designed for EEG emotion recognition tasks. It leverages graph convolutional operations to capture spatial dependencies between different electrodes in EEG signals. Graph Neural Networks, such as the DGCNN model, are essential for capturing and modeling relationships between graph-structured data, where nodes represent entities and edges represent connections. In the con- text of EEG emotion recognition, GNNs enable the DGCNN model to effectively learn and exploit the spatial dependencies between different electrodes. By leveraging graph convolutional operations, the DGCNN model can capture complex patterns and representations from EEG signals, leading to improved emotion recognition performance.

6. Results

6.1. Simulation Challenges in Maze Environment

In this section, we delve into the diverse simulation challenges encountered within the maze environment. These challenges are intentionally designed to assess the robot's capabilities and performance across various scenarios. An illustration showcasing the nine distinct challenges can be found in Figure.2.

6.2. Challenge 1: Square Maze

The first challenge introduces a straightforward square maze with the robot positioned at the center. This challenge serves as the baseline for assessing the robot's navigation capabilities.

6.3. Challenge 2: Square Maze with Dynamic Obstacles

Challenge 2 expands on the preceding challenge by incorporating four dynamic obstacles into the square maze. The introduction of these obstacles enhances the complexity of the robot's path planning and obstacle avoidance strategies.

6.4. Challenge 3: Varied Speed and Movement of Dynamic Obstacles

In this particular challenge, the dynamic obstacles showcase varying speeds and movement patterns in contrast to Challenge 2. The robot is required to adjust its navigation strategy accordingly to evade collisions.

6.5. Challenge 4: Maze with Inner Walls and Two Dynamic Obstacles

Challenge 4 integrates inner walls into the maze structure and introduces two dynamic obstacles. The inclusion of inner walls adds an additional layer of complexity to the robot's path planning process.

6.6. Challenge 5: Maze with Inner Walls and Six Dynamic Obstacles

This particular challenge incorporates inner walls; however, it introduces a higher number of dynamic obstacles, totaling six. This challenge is designed to assess the robot's capability to navigate through an environment with an increased density of obstacles.

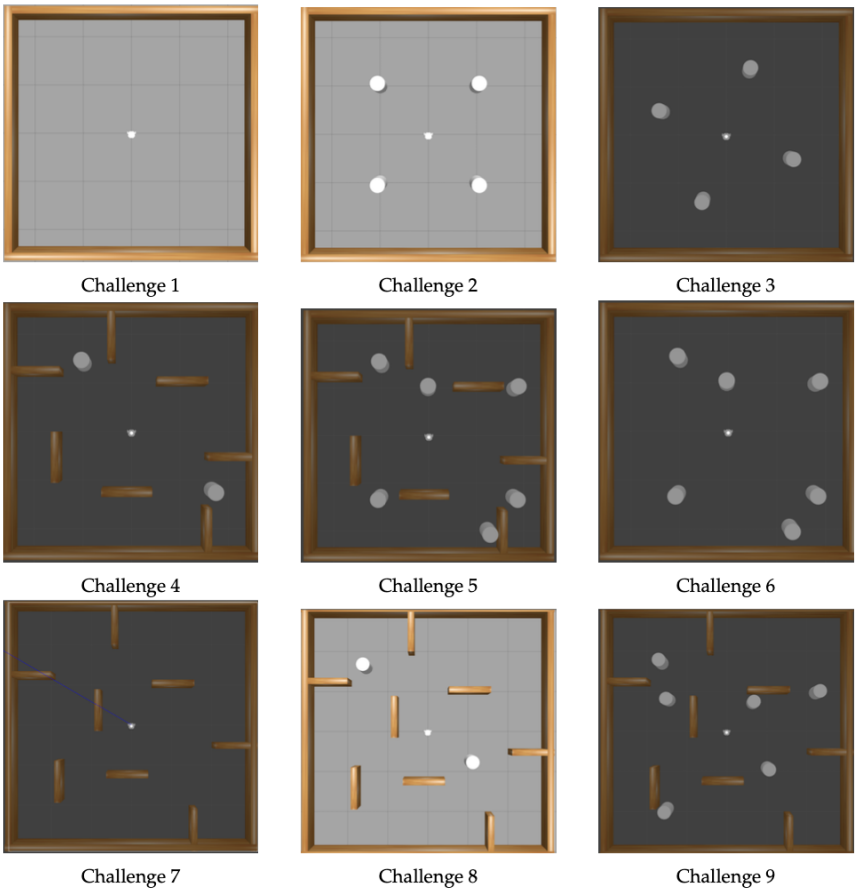

Figure 2: Challenges in Maze environment.

6.7. Challenge 6: Maze with Dynamic Obstacles (No Inner Walls)

Challenge 6 eliminates the inner walls present in Challenge 5 but retains the identical setup of six dynamic obstacles. This challenge assesses the robot's performance in navigating through an open maze environment.

6.8. Challenge 7: Larger Maze with More Inner Walls

Challenge 7 introduces a larger maze with a heightened count of inner walls. The robot is tasked with navigating through narrower passages and surmounting more intricate maze structures.

6.9. Challenge 8: Larger Maze with Inner Walls and Two Dynamic Obstacles

Expanding on the foundation set by Challenge 7, Challenge 8 introduces two dynamic obstacles to the maze. This challenge amalgamates the complexities of navigating in a larger maze with the additional challenge posed by moving obstacles.

6.10. Challenge 9: Larger Maze with Inner Walls and Six Dynamic Obstacles

Finally, Challenge 9 preserves the larger maze and inner walls featured in Challenge 8 but augments the number of dynamic obstacles to six. This challenge poses an exceptionally demanding scenario, evaluating the robot's capacity to navigate through intricate maze structures and contend with a high density of dynamic obstacles.

In summary, these nine challenges comprise a variety of maze configurations and obstacle arrangements, grad-

Model	Train Loss	Train Accuracy(%)	Validation Accuracy(%)	Test Accuracy(%)
CNN	0.0108 x 10^{-8}	27.54	26.87	28.32
LSTM	0.0062 x 10^{-8}	68.02	65.33	68.2
GRU	0.0063 x 10^{-8}	67.15	65.15	65.9
ViT	0.0003 x 10^{-8}	99.67	98.60	99.02
DQCNN	0.0001 x 10^{-8}	99.52	99.03	99.19

Table 1
Model performance

ually escalating in difficulty. Together, they facilitate a thorough assessment of the robot's navigation and obstacle avoidance capabilities. Figure.2 provides a visual representation of the different challenges discussed.

6.11. EEG Results

According to the provided table (Tab.6.11) displaying the outcomes of models trained on the SEED IV dataset, each model underwent training three times, and the average, as well as the variance of the scores, were computed. The DGCNN (Dynamic Graph Convolutional Neural Network) emerged as the top-performing model in terms of accuracy, delivering the most favorable results.

Specifically, DGCNN attained an average training accuracy of 99.52% and an average validation accuracy of 99.03%. In comparison, ViT (Vision Transformer) achieved an average training accuracy of 99.67% and an average validation accuracy of 98.60%.

The outstanding performance of DGCNN can be ascribed to its architectural features and capabilities. DGCNN employs graph convolutional layers, which adeptly capture and model intricate relationships and dependencies within the data. This renders it particularly suitable for tasks involving graph-structured data, such as the SEED IV dataset. Furthermore, the high accuracy demonstrated by DGCNN suggests its proficiency in generalizing effectively to unseen data.

In conclusion, the DGCNN model surpasses the other models in accuracy on the SEED IV dataset. The triumph of this model can be attributed to its architectural design and its capability to effectively capture complex relationships and dependencies within the data.

6.11.1. Analysis of DGCNN Training and Validation Results

Based on the training accuracy and validation accuracy plots of DGCNN [Fig.3], it is observed that the plots exhibit a synchronous pattern, with the training accuracy marginally surpassing the validation accuracy. Nevertheless, the validation plot does not deviate significantly from the training plot. This suggests that our model learns effectively, demonstrates good generalization, and exhibits stable learning in the initial epochs. The convergence of the plots becomes evident from epoch 80.

Additionally, the diminishing loss value as the model progresses through epochs indicates that the model is learning and refining its predictions. The training accuracy shows a consistent increase with each epoch, signifying an improvement in the model's ability to predict the training data. It commences at 48.08% and gradually advances to 99.26%.

Similarly, the validation accuracy follows a comparable trajectory to the training accuracy, initiating at 46.58% and progressing to 98.67%. This progression implies that the model effectively generalizes and maintains consistent performance on unseen data.

The final test accuracy also exhibits improvement over the epochs, commencing at 47.63% and culminating at 98.64%. This metric serves as a comprehensive gauge of the model's performance on the test set.

In summary, the training and validation accuracies of the DGCNN model exhibit a correlated movement, with the training accuracy marginally outperforming. The model showcases stable learning, begins convergence from epoch 80, and manifests enhancements in loss, training accuracy, validation accuracy, and final test accuracy over the epochs. These outcomes signify that the model learns effectively, generalizes proficiently, and attains high accuracy on both the training and validation datasets.

6.11.2. Analysis of Loss Curves and Convergence

Throughout the 100 epochs, both the loss curves of DGCNN exhibit minimal variance observed across multiple trials. This suggests that the model consistently converges towards similar local minima, yielding highly accurate predictions.

Furthermore, the loss curve illustrates a gradual descent, initiating from an initial high value and steadily decreasing throughout the training process. This indicates the model's effective learning and adjustment of its parameters to better fit the training data. After 100 epochs, DGCNN attains an impressive loss value of 0.0005, indicating a high level of accuracy and robust predictive capability.

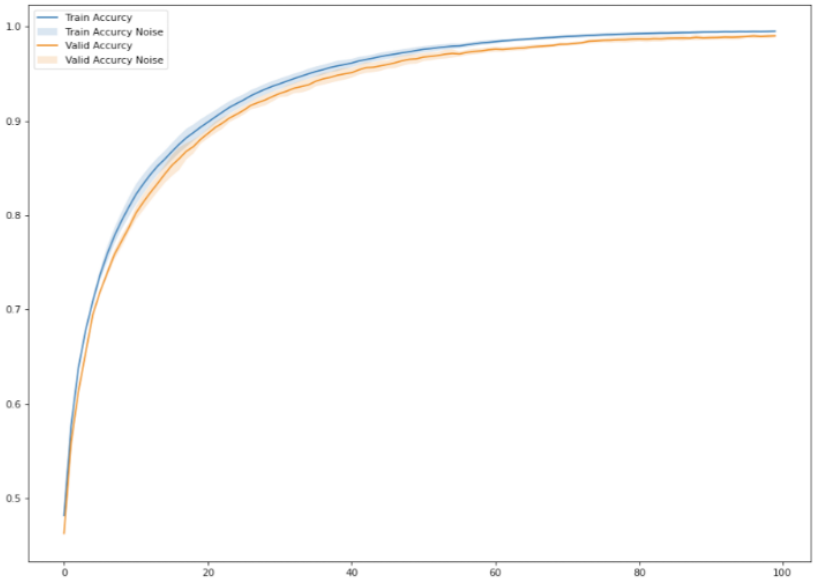

Figure 3: Train and Validation accuracy plots for 3 DGCNN model representing the average with variance.

This consistency underscores the stability and reliability of the solutions derived by DGCNN. In summary, the analysis of the loss curves of DGCNN unveils its remarkable capacity to minimize disparities between predictions and ground truth values, resulting in highly accurate models. DGCNN exhibits a robust ability to learn and converge towards dependable solutions, making it a valuable tool for various applications.

6.11.3. Analysis of Confusion Matrix

The confusion matrix provides valuable insights into the performance of classification models.

- Class 0 (Happiness):The DGCNN model achieves perfect accuracy (1.00) in classifying happiness, indicating no misclassifications in this category.
- Class 1 (Sadness): Similarly, the DGCNN model demonstrates flawless performance in identifying sadness, with a precision of 1.00.
- Class 2 (Fear): The DGCNN model performs well in detecting fear, with an accuracy of 0.98. However, it misclassifies a small portion (0.01) of the samples in this class as other emotions.
- Class 3 (Neutral): The DGCNN model achieves perfect accuracy (1.00) in recognizing neutral emotions, implying no misclassifications in this category.

The DGCNN model demonstrates outstanding classification outcomes, achieving perfect accuracies in recognizing happiness, sadness, and neutral emotions. It also performs commendably in detecting fear, with only a slight misclassification rate.

In conclusion, the DGCNN model showcases robust classification capabilities across all emotion classes. DGCNN delivers reliable predictions, establishing itself as a valuable tool for emotion classification tasks.

7. Conclusion

In this study, we conducted a thorough examination of the integration of deep reinforcement learning (DRL) with emotion feedback. Through a series of experiments, we identified optimal parameters to enhance learning outcomes by incorporating both lidar and emotion feedback. Our investigations yielded improved overall performance and a notable reduction in the number of episodes required for successful maze navigation. By incorporating natural sensor feedback, particularly human visual perception and brain signals, we gained valuable insights into the potential of utilizing such feedback in reinforcement learning tasks. Our findings highlight the effectiveness of combining deep reinforcement learning with emotion feedback, opening up new possibilities for leveraging natural sensor feedback and presenting opportunities for future work in multi-robot scenarios and transfer learning using brain signals beyond emotions.

Acknowledgments

This work has been developed at is.Lab() Intelligent Systems Laboratory at the Department of Computer, Control, and Management Engineering, Sapienza University of Rome (https:// islab.diag.uniroma1.it). The work has also been partially supported from Italian Ministerial grant PRIN 2022 "ISIDE: Intelligent Systems for Infrastructural Diagnosis in smart-concretE", n. 2022S88WAY - CUP B53D2301318, and by the Age-It: Ageing Well in an ageing society project, task 9.4.1 work package 4 spoke 9, within topic 8 extended partnership 8, under the National Recovery and Resilience Plan (PNRR), Mission 4 Component 2 Investment 1.3—Call for tender No. 1557 of 11/10/2022 of Italian Ministry of University and Research funded by the European Union—NextGenerationEU, CUP B53C22004090006.

References

[1] M. Khaled, B. Sirmaçek, S. Stramigioli, M. Poel, Towards continuous control for mobile robot navigation: A reinforcement learning and slam based approach, in: ISPRS Workshop Indoor 3D 2019, 2019.

[2] B. A. Nowak, R. K. Nowicki, M. Woźniak, C. Napoli, Multi-class nearest neighbour classifier for incomplete data handling, volume 9119, 2015, pp. 469 – 480. doi:10.1007/978-3-319-19324-3_42.

[3] H. Durrant-Whyte, T. Bailey, Simultaneous localization and mapping: part i, IEEE robotics & automation magazine 13 (2006) 99–110.

[4] L. Tai, G. Paolo, M. Liu, Virtual-to-real deep reinforcement learning: Continuous control of mobile robots for mapless navigation, in: 2017 IEEE/RSJ International Conference on Intelligent Robots and Systems (IROS), IEEE, 2017, pp. 31–36.

[5] Y. Zhu, R. Mottaghi, E. Kolve, J. J. Lim, A. Gupta, L. Fei-Fei, A. Farhadi, Target-driven visual navigation in indoor scenes using deep reinforcement learning, in: 2017 IEEE international conference on robotics and automation (ICRA), IEEE, 2017, pp. 3357–3364.

[6] J.-L. Qiu, X.-Y. Li, K. Hu, Correlated attention networks for multimodal emotion recognition, in: 2018 IEEE international conference on bioinformatics and biomedicine (BIBM), IEEE, 2018, pp. 2656–2660.

[7] G. De Magistris, R. Caprari, G. Castro, S. Russo, L. Iocchi, D. Nardi, C. Napoli, Vision-based holistic scene understanding for context-aware human-robot interaction, in: International Conference of the Italian Association for Artificial Intelligence, Springer, 2021, pp. 310–325.

[8] N. Brandizzi, S. Russo, G. Galati, C. Napoli, Addressing vehicle sharing through behavioral analysis: A solution to user clustering using recency-frequency-monetary and vehicle relocation based on neighborhood splits, volume 13, 2022. doi:10.3390/info13110511.

[9] E. Iacobelli, V. Ponzi, S. Russo, C. Napoli, Eye-tracking system with low-end hardware: Development and evaluation, Information 14 (2023) 644.

[10] K. Yao, T. Cohn, K. Vylomova, K. Duh, C. Dyer, Depth-gated recurrent neural networks, arXiv preprint arXiv:1508.03790 9 (2015) 98.

[11] Y.-T. Lan, W. Liu, B.-L. Lu, Multimodal emotion recognition using deep generalized canonical correlation analysis with an attention mechanism, in: 2020 International Joint Conference on Neural Networks (IJCNN), IEEE, 2020, pp. 1–6.

[12] I. E. Tibermacine, A. Tibermacine, W. Guettala, C. Napoli, S. Russo, Enhancing sentiment analysis on seed-iv dataset with vision transformers: A comparative study, in: Proceedings of the 2023 11th International Conference on Information Technology: IoT and Smart City, 2023, pp. 238–246.

[13] V. Ponzi, S. Russo, V. Bianco, C. Napoli, A. Wajda, Psychoeducative social robots for an healthier lifestyle using artificial intelligence: a case-study, volume 3118, 2021, pp. 26 – 33.

[14] B. Nail, M. A. Atoussi, S. Saadi, I. E. Tibermacine, C. Napoli, Real-time synchronisation of multiple fractional-order chaotic systems: An application study in secure communication, Fractal and Fractional 8 (2024) 104.

[15] S. Pepe, S. Tedeschi, N. Brandizzi, S. Russo, L. Iocchi, C. Napoli, Human attention assessment using a machine learning approach with gan-based data augmentation technique trained using a custom dataset, OBM Neurobiology 6 (2022). doi:10.21926/obm.neurobiol.2204139.

[16] A. Garulli, A. Giannitrapani, A. Rossi, A. Vicino, Mobile robot slam for line-based environment representation, in: Proceedings of the 44th IEEE Conference on Decision and Control, IEEE, 2005, pp. 2041–2046.

[17] V. Nguyen, A. Harati, A. Martinelli, R. Siegwart, N. Tomatis, Orthogonal slam: a step toward lightweight indoor autonomous navigation, in: 2006 IEEE/RSJ International Conference on Intelligent Robots and Systems, IEEE, 2006, pp. 5007–5012.

[18] E. H. C. Harik, A. Korsaeth, Combining hector slam and artificial potential field for autonomous navigation inside a greenhouse, Robotics 7 (2018) 22.

[19] G. Sepulveda, J. C. Niebles, A. Soto, A deep learning based behavioral approach to indoor autonomous navigation, in: 2018 IEEE international conference

on robotics and automation (ICRA), IEEE, 2018, pp. 4646–4653.
[20] Y.-H. Kim, J.-I. Jang, S. Yun, End-to-end deep learning for autonomous navigation of mobile robot, in: 2018 IEEE International Conference on Consumer Electronics (ICCE), IEEE, 2018, pp. 1–6.
[21] J. Wang, X. Ding, H. Xia, Y. Wang, L. Tang, R. Xiong, A lidar based end to end controller for robot navigation using deep neural network, in: 2017 IEEE International Conference on Unmanned Systems (ICUS), IEEE, 2017, pp. 614–619.
[22] B. Nail, B. Djaidir, I. E. Tibermacine, C. Napoli, N. Haidour, R. Abdelaziz, Gas turbine vibration monitoring based on real data and neuro-fuzzy system, Diagnostyka 25 (2024).
[23] S. Falciglia, F. Betello, S. Russo, C. Napoli, Learning visual stimulus-evoked eeg manifold for neural image classification, Neurocomputing (2024) 127654.
[24] A. Alfarano, G. De Magistris, L. Mongelli, S. Russo, J. Starczewski, C. Napoli, A novel convmixer transformer based architecture for violent behavior detection 14126 LNAI (2023) 3 – 16. doi:10.1007/978-3-031-42508-0_1.
[25] H. Quan, Y. Li, Y. Zhang, A novel mobile robot navigation method based on deep reinforcement learning, International Journal of Advanced Robotic Systems 17 (2020) 1729881420921672.
[26] P. Yue, J. Xin, H. Zhao, D. Liu, M. Shan, J. Zhang, Experimental research on deep reinforcement learning in autonomous navigation of mobile robot, in: 2019 14th IEEE Conference on Industrial Electronics and Applications (ICIEA), IEEE, 2019, pp. 1612–1616.
[27] X. Xue, Z. Li, D. Zhang, Y. Yan, A deep reinforcement learning method for mobile robot collision avoidance based on double dqn, in: 2019 IEEE 28th International Symposium on Industrial Electronics (ISIE), IEEE, 2019, pp. 2131–2136.
[28] X. Ruan, D. Ren, X. Zhu, J. Huang, Mobile robot navigation based on deep reinforcement learning, in: 2019 Chinese control and decision conference (CCDC), IEEE, 2019, pp. 6174–6178.
[29] H. Surmann, C. Jestel, R. Marchel, F. Musberg, H. Elhadj, M. Ardani, Deep reinforcement learning for real autonomous mobile robot navigation in indoor environments, arXiv preprint arXiv:2005.13857 (2020).
[30] P. Zhong, D. Wang, C. Miao, Eeg-based emotion recognition using regularized graph neural networks, IEEE Transactions on Affective Computing 13 (2020) 1290–1301.